Point mass identification in rectangular plates from minimal natural frequency data

Lourdes Rubio [a], José Fernández-Sáez [b], Antonino Morassi [c],*

[a] Department of Mechanical Engineering, University Carlos III of Madrid, Avda. de la Universidad 30, 28911 Leganés, Madrid, Spain
[b] Department of Continuum Mechanics and Structural Analysis, University Carlos III of Madrid, Avda. de la Universidad 30, 28911 Leganés, Madrid, Spain
[c] Dipartimento Politecnico di Ingegneria e Architettura, Università degli Studi di Udine, via Cotonificio 114, 33100 Udine, Italy

ARTICLE INFO

ABSTRACT

The inverse problem of determining the location and size of a point mass attached on a simply supported, isotropic and homogeneous rectangular plate from minimal natural frequency data is considered in this paper. Under the assumption that the size of the mass is small compared to the total mass of the plate, we show that the problem can be formulated and solved in closed form in terms of point mass-induced changes on the first three natural frequencies. Numerical simulations indicate that the method allows for accurate identification, provided that measurement/modelling errors are smaller than eigenfrequency changes.

© 2016 Elsevier Ltd. All rights reserved.

1. Introduction

The development of effective methods for timely identification of concentrated masses in vibrating plates is an issue of increasing interest in several fields of technology, such as, for instance, slabs supporting engines or motors not directly accessible from the exterior; printed circuits boards or plate-like chassis with electronic elements attached to them; plates with inhomogeneities in material mass density due to defective manufacturing processes; see, for example, the recent paper by Aydogdu and Filiz [1] and references cited therein. Moreover, in connection with the above applications, we also recall the possibility of using concentrated masses to modify the resonant frequencies of a thin uniform rectangular plate [2]. Ostachowicz et al. considered in [3] the interesting inverse problem of determining the location and size of a concentrated mass in a rectangular plate from natural frequency measurements. The authors used a class of optimization methods based on a genetic algorithm for solving the mass identification problem. The procedure was demonstrated on a simply supported rectangular plate made by linearly elastic isotropic and homogeneous material, and the first four natural frequencies were considered to construct the objective/error function to be minimized. In this paper we re-examine the problem by Ostachowicz et al. and, under the assumption that the size of the concentrated mass is small compared with the global mass of the plate, we derive a closed form solution based on natural frequency data. In particular, following a line of research on detection of defects in rods and beams (see, for instance, [4]), we carry out an identification based on a *minimal* set of natural frequencies. Since the unperturbed plate, as in [3], is completely known and a single point mass is attached, only three parameters need to be determined, namely the size of the mass and the two Cartesian coordinates of its location.

---

* Corresponding author.
  E-mail addresses: lrubio@ing.uc3m.es (L. Rubio), ppfer@ing.uc3m.es (J. Fernández-Sáez), antonino.morassi@uniud.it (A. Morassi).

Therefore, we investigate to what extent the measurement of the point mass-induced changes in the first three natural frequencies can be useful for mass identification.

Changes in natural frequencies are commonly used as concentrated mass indicators, since these data are relatively easy to measure with a satisfactory level of accuracy. However, the inverse problem formulated in terms of natural frequencies is intrinsically ill-posed, since, by the double symmetry of the unperturbed plate (i.e., the plate without point mass), a point mass located at any of a set of symmetrically placed points will produce identical changes in natural frequencies. This feature is confirmed by the symmetry of the objective function with respect to the mid-point axes of the rectangular plate found in [3]. Despite this ill-posedness of the inverse problem, we show that the linearized inverse problem can be solved in closed form from the knowledge of the changes in the first three natural frequencies, and the point mass can be uniquely localized up to a double symmetry location with respect to mid-point axes of the rectangular domain. The analysis also shows that a slightly different approach must be followed when the second eigenvalue of the unperturbed plate has double multiplicity, that is, for a square plate.

Our method is essentially based on the determination of an explicit expression of the sensitivity of a natural frequency to a single point mass (i.e., the first derivative with respect to the point mass size), and on the simple form that this expression takes in the case of a uniform, simply supported rectangular plate. The expression of the first derivative can be obtained for general domains and inhomogeneous anisotropic materials, following the lines of the classical perturbation theory of eigenvalues, see, for example, [5] and [6]. In particular, the analysis of the multiple eigenvalue case allowed us to give a theoretical justification of the interesting phenomenon observed, both numerically and experimentally, by Amabili et al. in [7], namely, the fact that a small mass placed on the diagonal of a square plate is enough to transform the shape of modes $(m = 1, n = 2)$ and $(m = 2, n = 1)$, where m and n are the number of half-waves in the two directions parallel to the plate sides, into vibrating modes with diagonal nodal lines.

The identification method has been tested on a series of numerical simulations. Numerical results support the theory in the absence of noise on the natural frequency data. The possible presence of measurement errors will result in a loss of accuracy in predicting the mass location and intensity, especially when the point mass is close to the boundary of the plate. The paper is organized as follows. The frequency sensitivity to a point mass is derived in Section 2 and it is specialized to simply supported rectangular plates in Section 3. The identification method is presented in Section 4. A selected set of results of numerical simulations is collected in Section 5.

2. Eigenpair sensitivity to a point mass

2.1. Formulation of the problem

Free transversal infinitesimal vibrations with radian frequency ω of a thin elastic clamped plate are governed by the boundary value problem

$$\begin{cases} M_{\alpha\beta,\alpha\beta}(u) + \lambda\rho u = 0, & \text{in } \Omega, \quad \text{(a)} \\ u = \dfrac{\partial u}{\partial n} = 0, & \text{on } \partial\Omega, \quad \text{(b)} \end{cases} \tag{1}$$

where Ω is a regular bounded domain in $\mathbb{R}^2$ coinciding with the middle-plane of the plate, n is the unit outer normal to $\partial\Omega$ and $u \in H_0^2(\Omega)$ describes the eigenfunction associated to the eigenvalue $\lambda = \omega^2$. Here, $H_0^2(\Omega)$ is the Hilbert space of the functions $f: \Omega \to \mathbb{R}$ such that f, the first and the second weak gradient of f are square summable on Ω, that is $\int_\Omega (f^2 + |\nabla f|^2 + |\nabla^2 f|^2) < \infty$, and the trace of f and of the gradient of f vanish on the boundary $\partial\Omega$. Moreover, hereinafter, repeated Greek indexes are assumed to be summed from 1 to 2. The plate is assumed to have no material damping, since its effect on the natural frequencies is known to be negligible. The quantities $M_{\alpha\beta}(u) = -P_{\alpha\beta\gamma\delta}u_{,\gamma\delta}$, $\alpha, \beta, \gamma, \delta = 1, 2$, and ρ denote the bending/torsional moments in a reference Cartesian system (O, X_1, X_2) and the mass density for unit area (of the middle plane) of the plate, respectively. The coefficients $P_{\alpha\beta\gamma\delta} = \frac{h^3}{12}C_{\alpha\beta\gamma\delta}$, $\alpha, \beta, \gamma, \delta = 1, 2$, are the Cartesian components of the plate tensor $\mathbb{P}$, where $\mathbb{C}$ is the elasticity tensor of the material and h is the uniform plate thickness. We shall be concerned with plates for which $\mathbb{P}$ satisfies:

(i) the minor and major symmetries, i.e., $P_{\alpha\beta\gamma\delta} = P_{\beta\alpha\gamma\delta} = P_{\alpha\beta\delta\gamma}$ and $P_{\alpha\beta\gamma\delta} = P_{\gamma\delta\alpha\beta}$;
(ii) $\mathbb{P}$ is a strongly convex fourth order tensor, i.e., $\mathbb{P}A \cdot A \geq \xi|A|^2$ in Ω for every 2×2 real symmetric matrix A, where $\xi > 0$ is a constant and $\cdot$ is the usual scalar product between second order tensors;
(iii) $\mathbb{P}$ belongs to $C^2(\overline{\Omega})$.

The function ρ will be assumed to be a continuous and strictly positive on $\overline{\Omega}$.

Vibration modes and corresponding natural frequencies are the eigensolutions of the boundary value problem (1a)–(1b), and we denote by $(u_n, \lambda_n = \omega_n^2)$, $n \geq 1$, the nth eigenpair of the *unperturbed* plate, that is the plate without the point mass. It is well-known that for such $\mathbb{P}$ and ρ, and under our assumptions on Ω, there exists an infinite sequence $\{\lambda_n\}_{n=1}^\infty$ of eigenvalues of (1a) and (1b) such that $0 < \lambda_1 \leq \lambda_2 \leq \lambda_3 \leq \ldots$, with $\lim_{n\to\infty}\lambda_n = \infty$; see [5]. Assume now that a point mass ϵ is attached at a

point P_0 belonging to the interior of Ω. The eigenvalue problem for the *perturbed* plate is the following

$$\begin{cases} M_{\alpha\beta,\alpha\beta}(\tilde{u}) + \tilde{\lambda}\tilde{\rho}\tilde{u} = 0, & \text{in } \Omega, \quad \text{(a)} \\ \tilde{u} = \dfrac{\partial\tilde{u}}{\partial n} = 0, & \text{on } \partial\Omega, \qquad \text{(b)} \end{cases} \qquad (2)$$

with

$$\tilde{\rho} = \rho + \epsilon\delta_{P_0}, \qquad (3)$$

where δ_{P_0} is Dirac's delta with support at P_0 and $\tilde{u} \in H_0^2(\Omega)$ is a nontrivial solution to (2a) and (2b) in the sense of distributions. To simplify the analysis, we introduce the following approximation of (3). Let $B_R(P_0) = \{x \in \Omega |\, |x - P_0| < R\} \subset\subset \Omega$, for R small enough, and consider the mass distribution

$$\tilde{\rho} = \rho + \epsilon(\delta\rho)(R), \quad (\delta\rho)(R) = \frac{\chi_{B_R(P_0)}}{|B_R(P_0)|}, \qquad (4)$$

where $\chi_{B_R(P_0)}$ is the characteristic function of the disc $B_R(P_0)$, i.e., $\chi_{B_R(P_0)}(x) = 1$ if $x \in B_R(P_0)$ and $\chi_{B_R(P_0)}(x) = 0$ otherwise, and $|B_R(P_0)| = area(B_R(P_0))$. The mass density $\tilde{\rho}$ converges to the function $\rho + \epsilon\delta_{P_0}$ as $R \to 0$ in the sense of distributions. Therefore, for a sufficiently small and given R, we replace (2a), (2b) and (3) with the following problem

$$\begin{cases} M_{\alpha\beta,\alpha\beta}(\tilde{u}) + \tilde{\lambda}(\rho + \epsilon(\delta\rho)(R))\tilde{u} = 0, & \text{in } \Omega, \quad \text{(a)} \\ \tilde{u} = \dfrac{\partial\tilde{u}}{\partial n} = 0, & \text{on } \partial\Omega, \qquad \text{(b)} \end{cases} \qquad (5)$$

where the perturbed eigenfunctions are denoted by the same symbol $\tilde{u}$. Also the plate problem (5a)–(5b) admits a countable sequence of eigenvalues $\{\tilde{\lambda}_n\}_{n=1}^{\infty}$ such that $0 < \tilde{\lambda}_1 \leq \tilde{\lambda}_2 \leq \tilde{\lambda}_3 \leq \dots$, with $\lim_{n\to\infty}\tilde{\lambda}_n = \infty$.

From general results of the variational theory of eigenvalues, it is known that an increase of the mass is attended by a prolongation of all the natural periods, or that no period can be diminished, i.e.,

$$\tilde{\lambda}_n \leq \lambda_n, \quad \text{for every } n \geq 1. \qquad (6)$$

On adopting the arguments shown in Jimbo et al. [8], one can prove that the eigenpairs of the perturbed plate $\{\tilde{\lambda}_n, \tilde{u}_n\}_{n=1}^{\infty}$ depend analytically on the perturbation parameter ϵ. More precisely, we have the following theorem, based on the general theory developed by Kato [6].

Theorem 2.1. *Under the above assumptions and notation, there exists $\hat{\epsilon}$, $\hat{\epsilon} > 0$, such that the eigenvalues $\tilde{\lambda}_n = \tilde{\lambda}_n(\epsilon)$ of the problem (5a)–(5b) are holomorphic functions of ϵ, for $0 < \epsilon < \hat{\epsilon}$. Moreover, there exists an orthonormal basis of $H_0^2(\Omega)$ (with respect to the standard scalar product) consisting of eigenfunctions of the problem (5a)–(5b), and these eigenfunctions are holomorphic functions of ϵ, for $0 < \epsilon < \hat{\epsilon}$.*

In order to formulate and solve the inverse problem, we derive an explicit expression of the first-order perturbation of the eigenvalues and eigenfunctions of the plate with respect to the parameter ϵ. To simplify the presentation, we introduce the following notation

$$Lu = M_{\alpha\beta,\alpha\beta}(u), \qquad (7)$$

where the operator L is self-adjoint in $H_0^2(\Omega)$, that is

$$\int_{\Omega}(Lf)g = \int_{\Omega}f(Lg), \quad \text{for every } f, g \in H_0^2(\Omega). \qquad (8)$$

The proof of (8) is standard and follows from integration by parts on using the major symmetry of the plate tensor $\mathbb{P}$. In our analysis, we distinguish two main cases, namely whether the unperturbed eigenvalues are simple or not.

2.2. Simple eigenvalues

Assume first that the unperturbed eigenvalue problem (1a)–(1b) has only simple eigenvalues, that is

$$(0 <)\lambda_1 < \lambda_2 < \dots < \lambda_n < \dots, \qquad (9)$$

with

$$dimX_{\lambda_n} = 1, \quad n = 1, 2, \dots, \qquad (10)$$

where X_{λ_n} is the eigenspace associated to the nth eigenvalue. By Theorem 2.1, the perturbed eigenvalues and the associated eigenfunctions can be expanded in convergent power series of the perturbation parameter ϵ, for $0 < \epsilon < \hat{\epsilon}$, where $\hat{\epsilon}$ is the number appearing in the statement of Theorem 2.1. Then, following Courant and Hilbert [5], we can write

$$\tilde{\lambda}_n = \lambda_n + \epsilon \mu_n + \epsilon^2 \nu_n + O(\epsilon^3), \tag{11}$$

$$\tilde{u}_n = u_n + \epsilon v_n + \epsilon^2 w_n + O(\epsilon^3), \tag{12}$$

for $0 < \epsilon < \hat{\epsilon}$, $n = 1, 2, \ldots$, where the real numbers μ_n, ν_n, ..., and the real-valued functions v_n, w_n belonging to $H_0^2(\Omega)$ have to be calculated. To simplify the analysis, we further assume that the μ_n's are all different, that is $\mu_n \neq \mu_k$ for every $n \neq k$, n, $k = 1, 2, \ldots$. Inserting (11) and (12) in (5a and 5b) and equating term by term, we obtain the following boundary value problem for the perturbation functions v_n and w_n:

$$\begin{cases} Lv_n + \lambda_n \rho v_n = -\mu_n \rho u_n - \lambda_n(\delta\rho)u_n, & \text{in } \Omega, \quad \text{(a)} \\ v_n = \dfrac{\partial v_n}{\partial n} = 0, & \text{on } \partial\Omega, \quad \text{(b)} \end{cases} \tag{13}$$

$$\begin{cases} Lw_n + \lambda_n \rho w_n = -\lambda_n(\delta\rho)v_n - \mu_n \rho v_n - \mu_n(\delta\rho)u_n - \nu_n \rho u_n, & \text{in } \Omega, \quad \text{(a)} \\ w_n = \dfrac{\partial w_n}{\partial n} = 0, & \text{on } \partial\Omega. \quad \text{(b)} \end{cases} \tag{14}$$

To simplify the notation, hereafter we write $(\delta\rho) = (\delta\rho)(R)$. In order to find v_n, we introduce its Fourier representation on the orthonormal basis $\{u_j\}_{j=1}^\infty$ of $H_0^2(\Omega)$:

$$v_n = \sum_{j=1}^\infty a_{nj} u_j, \quad a_{nj} = \int_\Omega \rho v_n u_j, \tag{15}$$

where $\int_\Omega \rho u_j u_k = \delta_{jk}$, j, $k = 1, 2, \ldots$. Here, δ_{jk} is the Kronecker symbol. By multiplying (13a) by u_l and integrating in Ω, recalling (8), we obtain

$$(\lambda_n - \lambda_l) \int_\Omega \rho v_n u_l = -\mu_n \delta_{nl} - \lambda_n \int_\Omega (\delta\rho)u_n u_l, \tag{16}$$

for n, $l = 1, 2, \ldots$. By taking $l=n$ in (16), we obtain

$$\mu_n = -\lambda_n \int_\Omega (\delta\rho)u_n^2, \quad n = 1, 2, \ldots \tag{17}$$

By taking $l \neq n$ in (16), we have

$$\int_\Omega \rho v_n u_l \equiv a_{nl} = -\frac{\lambda_n}{\lambda_n - \lambda_l} \int_\Omega (\delta\rho)u_n u_l, \quad n, l = 1, 2, \ldots, n \neq l. \tag{18}$$

The Fourier coefficient a_{nn} is found by the normalization condition on the perturbed eigenfunction $\tilde{u}_n$, with respect to the (known) unperturbed mass distribution ρ, namely

$$1 = \int_\Omega \rho \tilde{u}_n^2. \tag{19}$$

Inserting the Taylor expansion (12) in (19), we find

$$\int_\Omega \rho v_n u_n \equiv a_{nn} = 0, \quad n = 1, 2, \ldots \tag{20}$$

In conclusion, we have

$$v_n = \sum_{j=1, j \neq n}^\infty \frac{d_{nj}}{\lambda_n - \lambda_j} u_j, \tag{21}$$

where

$$d_{nj} = -\lambda_n \int_\Omega (\delta\rho)u_n u_j, \quad n, j = 1, 2, \ldots, n \neq j. \tag{22}$$

Second order approximations can be determined similarly. Multiplying (14a) by u_k and integrating by parts we obtain

$$(\lambda_n - \lambda_k) \int_\Omega \rho w_n u_k = -\lambda_n \int_\Omega (\delta\rho)v_n u_k - \mu_n \int_\Omega \rho v_n u_k - \mu_n \int_\Omega (\delta\rho)u_n u_k - \nu_n \delta_{nk}, \tag{23}$$

for n, $k = 1, 2, \ldots$.

Setting $k=n$ in the above identity and recalling (20), we have

$$\nu_n = -\lambda_n \int_\Omega (\delta\rho) v_n u_n - \mu_n \int_\Omega (\delta\rho) u_n^2, \quad n = 1, 2, \ldots \tag{24}$$

For $k \neq n$, we can find the Fourier coefficients of w_n on the basis $\{u_k\}_{k=1}^\infty$:

$$\int_\Omega \rho w_n u_k = -\frac{1}{\lambda_n - \lambda_k}(\lambda_n \int_\Omega (\delta\rho) v_n u_k + \mu_n \int_\Omega (\rho v_n u_k + (\delta\rho) u_n u_k)), \tag{25}$$

for $n, k = 1, 2, \ldots, k \neq n$. The remaining Fourier coefficient $\int_\Omega \rho w_n u_n$ can be found by using once more the normalization condition (19):

$$\int_\Omega \rho w_n u_n = -\frac{1}{2}\int_\Omega \rho v_n^2, \quad n = 1, 2, \ldots \tag{26}$$

2.3. Multiple eigenvalues

We now consider the case of multiple eigenvalues. Without loss of generality and only for simplicity, we assume that the first eigenvalue of the unperturbed eigenvalue problem (1) is α-fold, $\alpha \geq 2$, whereas for $j > \alpha$ the remaining eigenvalues are simple, that is

$$(0 <)\lambda_1 = \lambda_2 = \cdots = \lambda_\alpha \equiv \lambda < \lambda_{\alpha+1} < \cdots < \lambda_n < \cdots \tag{27}$$

It is known that the dimension of the eigenspace X_λ and X_{λ_n} associated with λ and λ_n, respectively, is given by

$$dim(X_\lambda) = \alpha, \quad dim(X_{\lambda_n}) = 1, \quad n = \alpha + 1, \alpha + 2, \ldots \tag{28}$$

We denote by $\{u_n\}_{n=1}^\alpha$ a given orthonormal basis of X_λ. For $j > \alpha$, the analysis presented for simple eigenvalues is still valid. Therefore, we only need to consider $n = 1, \ldots, \alpha$. In this case, a supplementary discussion is needed. If λ is a multiple eigenvalue of the perturbed problem, then the corresponding eigenfunctions are determined by an orthogonal transformation. In fact, any family of functions obtained as a (no singular) linear combination of $\{u_j\}_{j=1}^\alpha$, say $\{u_k^* = \sum_{j=1}^\alpha c_{kj}u_j\}_{k=1}^\alpha$, for real coefficients c_{kj} such that $\det(c_{kj}) \neq 0$, still is a family of eigenfunctions for the α-fold eigenvalue λ. In particular, by imposing the orthonormalization condition on u_k^*, we obtain

$$\delta_{kl} = \int_\Omega \rho u_k^* u_l^* = \sum_{r,s=1}^\alpha c_{kr}c_{ls}\int_\Omega \rho u_r u_s = \sum_{r,s=1}^\alpha c_{kr}c_{ls}\delta_{rs} = \sum_{r,s=1}^\alpha c_{kr}c_{lr}, \tag{29}$$

or, equivalently, $cc^T = 1_\alpha$, where 1_α is the $\alpha \times \alpha$ identity matrix, namely (c_{kj}) is an orthogonal transformation.

Basing on the above considerations, it is evident that we cannot expect the individual eigenfunctions $\{\tilde{u}_j\}_{j=1}^\alpha$ to vary continuously with the parameter ϵ, unless the system of unperturbed eigenfunctions $\{u_j^*\}_{j=1}^\alpha$ (i.e., the orthogonal matrix c) has been selected in a proper way. In fact, Theorem 2.1 guarantees for the existence of such a basis. Therefore, we introduce the orthogonal transformation

$$u_n^* = \sum_{j=1}^\alpha \gamma_{nj}u_j, \quad n = 1, \ldots, \alpha, \tag{30}$$

where the orthogonal matrix (γ_{nj}) will be determined later. By Theorem 2.1, we consider the following power series expansion in a neighborhood of (λ_n, u_n^*)

$$\tilde{\lambda}_n = \lambda_n + \epsilon\mu_n + \epsilon^2\nu_n + O(\epsilon^3), \tag{31}$$

$$\tilde{u}_n = u_n^* + \epsilon v_n + \epsilon^2 w_n + O(\epsilon^3), \tag{32}$$

for $0 < \epsilon < \hat{\epsilon}$, $n = 1, 2, \ldots, \alpha$, where the real numbers $\mu_n, \nu_n, \ldots$ and the real-valued functions v_n, w_n belonging to $H_0^2(\Omega)$ have to be determined. By inserting (31) and (32) in (5a and 5b), we find

$$\begin{cases} Lv_n + \lambda_n\rho v_n = -\mu_n\rho\sum_{j=1}^\alpha \gamma_{nj}u_j - \lambda_n(\delta\rho)\sum_{j=1}^\alpha \gamma_{nj}u_j, & \text{in } \Omega, \quad \text{(a)} \\ v_n = \dfrac{\partial v_n}{\partial n} = 0, \quad \text{on } \partial\Omega, & \qquad\qquad\text{(b)} \end{cases} \tag{33}$$

$$\begin{cases} Lw_n + \lambda_n\rho w_n = -\lambda_n(\delta\rho)v_n - \mu_n\rho v_n - (\mu_n(\delta\rho) + \nu_n\rho)\sum_{j=1}^\alpha \gamma_{nj}u_j, & \text{in } \Omega, \quad \text{(a)} \\ w_n = \dfrac{\partial w_n}{\partial n} = 0, \quad \text{on } \partial\Omega. & \qquad\qquad\text{(b)} \end{cases} \tag{34}$$

By proceeding as before, we multiply (33a) by u_l, $l \geq 1$, and integrate by parts on Ω, obtaining

$$(\lambda_n - \lambda_l) \int_\Omega \rho v_n u_l = - \sum_{j=1}^{\alpha} (\mu_n \delta_{jl} + \lambda_n \int_\Omega (\delta \rho) u_j u_l) \gamma_{nj}, \tag{35}$$

for $n = 1, 2, ..., \alpha$, $l = 1, 2, ..., \alpha, \alpha + 1, ...$

If $l = 1, 2, ..., \alpha$, then the left hand side of (35) vanishes, and we have

$$\sum_{j=1}^{\alpha} (d_{jl} - \mu_n \delta_{jl}) \gamma_{nj} = 0, \quad d_{jl} = - \lambda \int_\Omega (\delta \rho) u_j u_l, \quad l, n = 1, ..., \alpha. \tag{36}$$

This is the eigenvalue problem for the real symmetric $\alpha \times \alpha$ matrix (d_{jl}) and, for every given n, $n = 1, ..., \alpha$, the vector $\gamma^{(n)} = \{\gamma_{nj}\}_{j=1}^{\alpha}$ (i.e., the nth row of the matrix γ) is the eigenvector associated to the eigenvalue μ_n. Therefore, the first order changes $\{\mu_n\}_{n=1}^{\alpha}$ and the orthogonal matrix γ are uniquely determined.

By the formulation (36) it is clear that the first order variations of the eigenvalues do not depend on the original choice of the orthonormal basis of X_λ. In fact, let $(q_{jl})_{j,l=1}^{n}$ be another transformation and consider

$$u_n^{**} = \sum_{l=1}^{\alpha} q_{nl} u_l, \quad n = 1, ..., \alpha. \tag{37}$$

Then, by repeating the above arguments and using (30), we obtain an eigenvalue problem analogous to (36), namely (in compact notation)

$$(S - \mu^{**} 1) v = 0, \tag{38}$$

where the $\alpha \times \alpha$ matrix S is given by

$$S = (q\gamma^{-1}) d (q\gamma^{-1})^{-1}, \tag{39}$$

where γ^{-1} is the inverse of γ. From Eq. (39), the eigenvalue problems (36) and (38) clearly have the same eigenvalues.

The second order changes of the eigenvectors and eigenvalues can be obtained as before, see, for example, [8] for details.

2.4. Frequency sensitivity to a point mass

To conclude the analysis of Section 2, we specialize the first order eigenvalue change formula to the case of a point mass. In case of simple eigenvalues, by (17) and (4) we have

$$\mu_n = - \frac{\lambda_n}{|B_R(P_0)|} \int_{B_R(P_0)} u_n^2, \quad \text{for every small enough and positive } R. \tag{40}$$

By the regularity of u_n ($u_n \in C(\overline{\Omega})$) and taking the limit in (40) as $R \to 0$, we have

$$\delta \lambda_n \equiv \epsilon \mu_n = - \epsilon \lambda_n u_n^2(P_0). \tag{41}$$

Therefore, the change in a (squared) natural frequency produced by a single point mass ϵ may be expressed in this case as the product of three quantities: the (squared) natural frequency itself, the square of the corresponding mode shape of the unperturbed plate evaluated at the mass position, and the mass variation ϵ. Note that the first order eigenvalue change vanishes on a nodal curve of the unperturbed mode shape. Expression (41) is the two-dimensional version of the first-order eigenvalue change found in [9] for rods and beams, see also the analysis developed in [10].

For an eigenvalue λ with multiplicity $\alpha \geq 2$, the matrix $(d_{jl})_{j,l=1}^{\alpha}$ appearing in (36) and associated to a point mass ϵ placed in P_0 is given by

$$d_{jl} = \lim_{R \to 0} (-\lambda \int_\Omega \frac{\chi_{B_R(P_0)}}{|B_R(P_0)|} u_j u_l) = - \lambda u_j(P_0) u_l(P_0), \tag{42}$$

that is, in compact notation,

$$d = - \lambda \eta(P_0) \otimes \eta(P_0), \tag{43}$$

where $\eta(P_0) = (u_1(P_0), ..., u_\alpha(P_0))$ is the α-vector whose kth component is equal to the value of the kth eigenfunction at P_0. We recall that, given two α-vectors a and b, the $\alpha \times \alpha$ matrix $a \otimes b$ appearing in (43) is defined as $(a \otimes b)_{jl} = a_j b_l$, $j, l = 1, ..., \alpha$. By (43), if $\eta(P_0) = 0$, then $\mu_n = 0$ for every $n = 1, ..., \alpha$, and we can consider the canonical basis $\{\gamma^{(i)} = e_i\}_{i=1}^{\alpha}$ as the orthonormal basis of eigenvectors of the eigenvalue problem (36). Conversely, if $\eta(P_0) \neq 0$, then we find the following eigenpairs:

$$\mu_1 = - \lambda |\eta(P_0)|^2, \quad \text{with normalized eigenvector } \gamma^{(1)} = \frac{\eta(P_0)}{|\eta(P_0)|}, \tag{44}$$

$$\mu_2 = \ldots = \mu_\alpha = 0, \quad \text{with } (\alpha - 1) \text{ eigenvectors orthonormal to } \eta(P_0), \ \{\gamma^{(i)}\}_{i=2}^\alpha. \tag{45}$$

3. Application of the sensitivity analysis to rectangular simply supported uniform plates

In the previous section we have derived the first-order change in the eigenvalues induced by an additional small mass placed in an interior point of a plate clamped at the boundary. By analyzing the steps that led to expressions (41)–(42), it is clear that the procedure can be extended to any set of boundary conditions. In this section we examine closely the sensitivity equations for rectangular simply supported uniform plates. The case is simple but significative, and largely applied in practice, see, for instance, [3]. Moreover, it is one of the few situations in which closed-form expressions of the eigenpairs are available. Let the plate be made by linearly elastic, homogeneous and isotropic material, with Young's modulus E, $E > 0$, and Poisson's coefficient ν, $\nu \in (0, \frac{1}{2})$. Let us denote by $D = \frac{Eh^3}{12(1-\nu^2)}$ the bending stiffness of the plate, where h is the constant thickness. Let Ω be the rectangle $(0, a) \times (0, b)$ in a two-dimensional reference cartesian system of origin $O = (0, 0)$ and axis (X,Y). The infinitesimal undamped free vibration of the unperturbed plate are governed by the following eigenvalue problem

$$\begin{cases} D\Delta^2 u - \lambda \rho u = 0, & \text{in } \Omega, & \text{(a)} \\ u = \dfrac{\partial^2 u}{\partial x^2} = 0, & \text{on } x = 0 \text{ and on } x = a, & \text{(b)} \\ u = \dfrac{\partial^2 u}{\partial y^2} = 0, & \text{on } y = 0 \text{ and on } y = b. & \text{(c)} \end{cases} \tag{46}$$

The (n,m)th normalized eigenpair of the unperturbed plate is

$$\omega_{nm}^2 = \lambda_{nm} = \frac{\pi^4 D}{\rho}\left(\left(\frac{n}{a}\right)^2 + \left(\frac{m}{b}\right)^2\right)^2, \quad u_{nm}(x, y) = \frac{2}{\sqrt{\rho ab}} \sin \frac{n\pi x}{a} \sin \frac{m\pi y}{b}, \tag{47}$$

for $n, m \geq 1$. Assume that a and b are chosen so that the "lower" eigenvalues are simple, i.e., if, for example, $\frac{b}{a} = \frac{5}{4}$, then the first eight eigenvalues are simple. Then, Eq. (41) gives

$$\delta\lambda_{nm} = -\epsilon \frac{4\pi^4 D}{\rho^2 ab}\left(\left(\frac{n}{a}\right)^2 + \left(\frac{m}{b}\right)^2\right)^2 \sin^2 \frac{n\pi x_0}{a} \sin^2 \frac{m\pi y_0}{b}, \tag{48}$$

where $P_0 = (x_0, y_0)$.

As an example of plate with multiple eigenvalues, we consider in detail the case of a square plate, namely $a=b$. The eigenvalues are given by

$$\lambda_{nm} = \frac{\pi^4 D}{\rho a^4}(n^2 + m^2)^2, \quad n, m \geq 1, \tag{49}$$

and, therefore, those with $n=m$ are simple, whereas the other have multiplicity $\alpha = 2$. Under the notation of the previous section and for $n \neq m$, let

$$\left\{ u_1 = \frac{2}{a\sqrt{\rho}} \sin \frac{n\pi x}{a} \sin \frac{m\pi y}{a}, \ u_2 = \frac{2}{a\sqrt{\rho}} \sin \frac{m\pi x}{a} \sin \frac{n\pi y}{a} \right\} \tag{50}$$

be an orthonormal basis of the eigenspace $X_{\lambda=\lambda_{nm}}$. Moreover, let

$$\eta(P_0) = (u_1(P_0), u_2(P_0)) \tag{51}$$

and, avoiding the trivial case, we assume $\eta(P_0) \neq 0$. Then, the eigenvalue problem (36) has eigensolutions

$$\left(\mu_1 = -\lambda |\eta(P_0)|^2, \ \gamma^{(1)} = (\gamma_{1j})_{j=1}^2 = \frac{(u_1(P_0)), u_2(P_0))}{|\eta(P_0)|} \right), \tag{52}$$

$$\left(\mu_2 = 0, \ \gamma^{(2)} = (\gamma_{2j})_{j=1}^2 = \frac{(-u_2(P_0), u_1(P_0))}{|\eta(P_0)|} \right), \tag{53}$$

and the orthogonal matrix γ is uniquely determined. We conclude the analysis of the square plate with a couple of examples.

Example 1. Let $n=1$, $m=2$, $x_0 = y_0$, with $x_0 \neq \frac{a}{2}$. We have:

$$\eta(P_0) = \frac{2}{a\sqrt{\rho}} \sin \frac{\pi x_0}{a} \sin \frac{2\pi x_0}{a}(1, 1) \tag{54}$$

and

$$\left\{ \mu_1 = -\frac{8\lambda}{\rho a^2} \sin^2 \frac{\pi x_0}{a} \sin^2 \frac{2\pi x_0}{a}, \; \gamma^{(1)} = \frac{1}{\sqrt{2}}(1, 1) \right\},$$ (55)

$$\{ \mu_2 = 0, \; \gamma^{(2)} = \frac{1}{\sqrt{2}}(-1, 1) \},$$ (56)

$$\gamma = \frac{1}{\sqrt{2}} \begin{pmatrix} 1 & 1 \\ -1 & 1 \end{pmatrix}.$$ (57)

Then, by (30), we have

$$u_1^* = \frac{8}{a\sqrt{2\rho}} \sin \frac{\pi x}{a} \sin \frac{\pi y}{a} \cos \frac{\pi(x+y)}{2a} \cos \frac{\pi(x-y)}{2a}$$ (58)

and

$$u_2^* = -\frac{8}{a\sqrt{2\rho}} \sin \frac{\pi x}{a} \sin \frac{\pi y}{a} \sin \frac{\pi(x+y)}{2a} \sin \frac{\pi(x-y)}{2a}$$ (59)

We notice that, inside Ω,

$$u_1^* = 0 \Leftrightarrow y = a - x, \quad u_2^* = 0 \Leftrightarrow y = x,$$ (60)

whereas the nodal lines of the initial basis $\{u_1, u_2\}$ coincide with the segments of Ω of equation $x_1 = \frac{a}{2}$ and $x_2 = \frac{a}{2}$. The new basis of X_λ is $\{u_1^*, u_2^*\}$ and, since $u_1^*(x_0, x_0) \neq 0$ and $u_2^*(x_0, x_0) = 0$, we obtain $\mu_1 \neq 0$, $\mu_2 = 0$ (see (55) and (56)).

Basing on the above calculations, we can state that the addition of a (even) small point mass at $(x_0, y_0 = x_0)$, $x_0 \neq \frac{a}{2}$, has the effect of redirecting the original basis $\{u_1, u_2\}$ of the eigenspace X_λ by rotating of $\frac{\pi}{4}$ the nodal lines. This fact was recently pointed out in the experimental and numerical investigation developed by Amabili et al. [7] on the effect of rotary inertia of an attached mass in the eigenparameters of a square plate. Finally, if $x_0 = y_0 = \frac{a}{2}$, then the first order changes of the eigenvalue λ_{12} vanish.

Example 2. We consider, as before, $n=1$ and $m=2$, but in this example we not necessarily assume $x_0 = y_0$. To avoid the trivial situation, let $(x_0, y_0) \neq (\frac{a}{2}, \frac{a}{2})$. We have

$$\eta(P_0) = \frac{2}{a\sqrt{\rho}} \left(\sin \frac{\pi x_0}{a} \sin \frac{2\pi y_0}{a}, \sin \frac{2\pi x_0}{a} \sin \frac{\pi y_0}{a} \right)$$ (61)

and, therefore,

$$\mu_1 = -\frac{4\lambda}{\rho a^2} \left(\sin^2 \frac{\pi x_0}{a} \sin^2 \frac{2\pi y_0}{a} + \sin^2 \frac{2\pi x_0}{a} \sin^2 \frac{\pi y_0}{a} \right),$$ (62)

$$\gamma^{(1)} = C \left(\sin \frac{\pi x_0}{a} \sin \frac{2\pi y_0}{a}, \sin \frac{2\pi x_0}{a} \sin \frac{\pi y_0}{a} \right),$$ (63)

$$\left\{ \mu_2 = 0, \gamma^{(2)} = C \left(-\sin \frac{2\pi x_0}{a} \sin \frac{\pi y_0}{a}, \sin \frac{\pi x_0}{a} \sin \frac{2\pi y_0}{a} \right) \right\},$$ (64)

where $C \neq 0$ is a normalization constant, and

$$\gamma = \frac{1}{\sqrt{2}} \begin{pmatrix} \gamma_1^{(1)} & \gamma_2^{(1)} \\ \gamma_1^{(2)} & \gamma_2^{(2)} \end{pmatrix}.$$ (65)

Finally, by (30) and after a rearrangement of the terms, we have

$$u_1^* = C' \sin \frac{\pi x_0}{a} \sin \frac{\pi x}{a} \sin \frac{\pi y_0}{a} \sin \frac{\pi y}{a} \left(\cos \frac{\pi y_0}{a} \cos \frac{\pi y}{a} + \cos \frac{\pi x_0}{a} \cos \frac{\pi x}{a} \right)$$ (66)

and

$$u_2^* = C' \sin \frac{\pi x_0}{a} \sin \frac{\pi x}{a} \sin \frac{\pi y_0}{a} \sin \frac{\pi y}{a} \left(\cos \frac{\pi y_0}{a} \cos \frac{\pi x}{a} - \cos \frac{\pi x_0}{a} \cos \frac{\pi y}{a} \right),$$ (67)

where $C' \neq 0$ is a normalization constant. We notice that

$$u_1^*(P_0) \neq 0, \quad u_2^*(P_0) = 0. \tag{68}$$

4. Identification of a point mass in a simply supported rectangular plate

Eq. (41) has an important consequence: the ratios of the relative changes in two different natural frequencies depend only on the location of the point mass $P_0 = (x_0, y_0) \in \Omega$, not on its magnitude ϵ, that is (denoting the eigenvalues by a single index, for simplicity of notation)

$$\frac{\frac{\delta\lambda_n}{\lambda_n}}{\frac{\delta\lambda_m}{\lambda_m}} = \frac{u_n^2(x_0, y_0)}{u_m^2(x_0, y_0)} \equiv f(x_0, y_0), \tag{69}$$

where $\delta\lambda_m < 0$. Note that if $\delta\lambda_m = 0$, then the possible point mass locations coincide with the nodal curves of the mth vibrating mode u_m of the unperturbed plate. The problem related to the point mass location consists in determining the solutions of (69) for a fixed-measured value of the ratio $(\delta\lambda_n/\lambda_n)/(\delta\lambda_m/\lambda_m)$. It follows from (69) that all and the only possible location of the point mass are the points (x_0, y_0) of the function $f(x, y) = (u_n(x, y)/u_m(x, y))^2$ graph intersecting with the horizontal plane drawn parallel to the plane (x,y) at a distance equal to the ratio $(\delta\lambda_n/\lambda_n)/(\delta\lambda_m/\lambda_m)$. These intersections generally are curves on the plane (x,y) and, in order to reduce the indeterminacy, another or more equations as (69) can be considered, depending on the measurements available. On a practical level, once the free vibration problem related to the unperturbed plate is solved, the behavior of $f(x, y)$ is known and, therefore, it is possible, via a numerical procedure for example, to determine the solutions of (69). We shall see in the sequel that there are situations important in applications in which the effects of non-uniqueness of the solution may be considerably reduced by means of a careful choice of the data.

Let us consider first the case of a simply supported rectangular plate $\Omega = (0, a) \times (0, b)$ having first three eigenvalues simple. By (41) and recalling (47), we have

$$C_{11} \equiv -\frac{\delta\lambda_{11}}{C\lambda_{11}} = \epsilon \ \sin^2 \frac{\pi x_0}{a} \ \sin^2 \frac{\pi y_0}{b}, \tag{70}$$

$$C_{12} \equiv -\frac{\delta\lambda_{12}}{C\lambda_{12}} = \epsilon \ \sin^2 \frac{\pi x_0}{a} \ \sin^2 \frac{2\pi y_0}{b}, \tag{71}$$

$$C_{21} \equiv -\frac{\delta\lambda_{21}}{C\lambda_{21}} = \epsilon \ \sin^2 \frac{2\pi x_0}{a} \ \sin^2 \frac{\pi y_0}{b}, \tag{72}$$

where $C = \frac{4}{\rho ab}$.

We prove that the measurement of the triple $\{C_{11}, C_{12}, C_{21}\}$ determines uniquely the intensity ϵ of the point mass and the variables $S = \cos \frac{2\pi x_0}{a}$, $T = \cos \frac{2\pi y_0}{b}$ of the point mass location (x_0, y_0).

The crucial point is that the first eigenfunction u_{11} never vanishes inside Ω. This means that the first eigenvalue is always sensitive to the point mass or, equivalently, $C_{11} > 0$ for every $P_0 \in \Omega$. Then, we can consider the ratio C_{12}/C_{11}. Using standard trigonometric identities, we easily get

$$T = \frac{C_{12}}{2C_{11}} - 1. \tag{73}$$

Similarly, we can consider the ratio C_{21}/C_{11} obtaining

$$S = \frac{C_{21}}{2C_{11}} - 1. \tag{74}$$

Once the variable positions T and S are determined, the mass intensity can be evaluated, for example, by introducing (73) and (74) in (70):

$$\epsilon = \frac{4C_{11}}{(1 - T)(1 - S)}. \tag{75}$$

We have shown that the knowledge of the frequency changes of the first three vibration modes allows us to uniquely determine the point-mass variation ϵ, and the point-mass coordinates (x_0, y_0), up to symmetric positions with respect to the symmetry axes $x = \frac{a}{2}$, $y = \frac{b}{2}$. In fact, let us denote by x_0^-, x_0^+ the two solutions of (74) in $(0, a)$, with $x_0^- < x_0^+$ and $x_0^- + x_0^+ = a$. Similarly, let y_0^-, y_0^+, with $y_0^- < y_0^+$ and $y_0^- + y_0^+ = b$, be the two solutions of (73) in $(0, b)$. Then, the complete set of possible positions of the point mass in the rectangular plate $(0, a) \times (0, b)$ is $\{(x_0^-, y_0^-), (x_0^-, y_0^+), (x_0^+, y_0^-), (x_0^+, y_0^+)\}$.

We now consider the identification of the point mass in a simply supported plate with multiple eigenvalues and, for simplicity of the presentation, we assume $a=b$ (square plate). The eigenvalues λ_{11} and λ_{22} are simple, whereas λ_{12} has
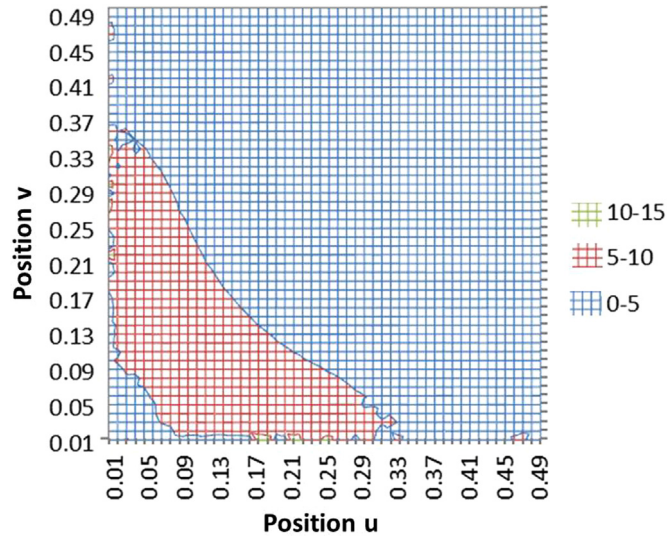
Fig. 1. Percentage error in mass identification for mass size equal to 0.25% of the mass plate.

multiplicity 2, see Section 3. Therefore, by (41), (62)–(64), we have

$$C_{11} \equiv -\frac{\delta\lambda_{11}}{C\lambda_{11}} = \epsilon \, \sin^2 \frac{\pi x_0}{a} \, \sin^2 \frac{\pi y_0}{a}, \tag{76}$$

$$C_{12} \equiv -\frac{\delta\lambda_{12}}{C\lambda_{12}} = \epsilon \left(\sin^2 \frac{\pi x_0}{a} \, \sin^2 \frac{2\pi y_0}{a} + \sin^2 \frac{2\pi x_0}{a} \, \sin^2 \frac{\pi y_0}{a} \right), \tag{77}$$

$$C_{22} \equiv -\frac{\delta\lambda_{22}}{C\lambda_{22}} = \epsilon \, \sin^2 \frac{2\pi x_0}{a} \, \sin^2 \frac{2\pi y_0}{a}, \tag{78}$$

where $C = \frac{4}{\rho a^2}$. As before, $C_{11} > 0$ for every position of the mass inside Ω. The frequency shift C_{12} vanishes if and only if $x_0 = y_0 = \frac{a}{2}$, and $C_{22} = 0$ if and only if either $x_0 = \frac{a}{2}$ or $y_0 = \frac{a}{2}$. Without loss of generality, we can assume $C_{12} > 0$. (If $C_{12} = 0$, then the mass is located at $x_0 = y_0 = \frac{a}{2}$, and the mass magnitude ϵ can be determined by (76).) Then, by (77) and (78), we have
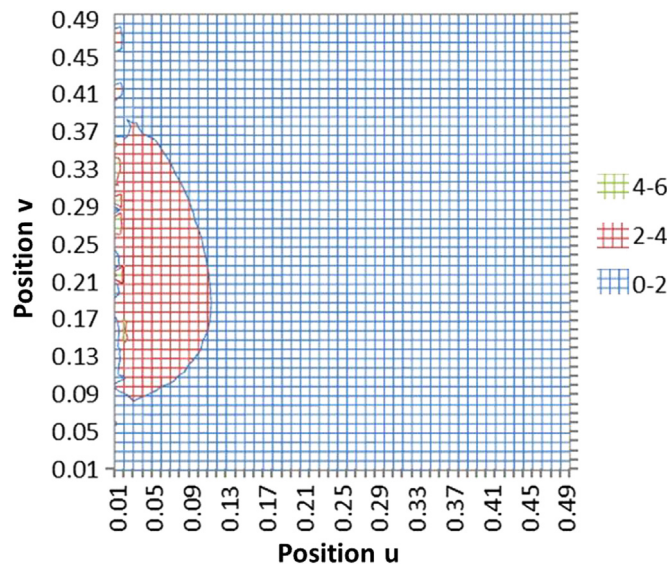
Fig. 2. Percentage error in position u for mass size equal to 0.25% of the mass plate.
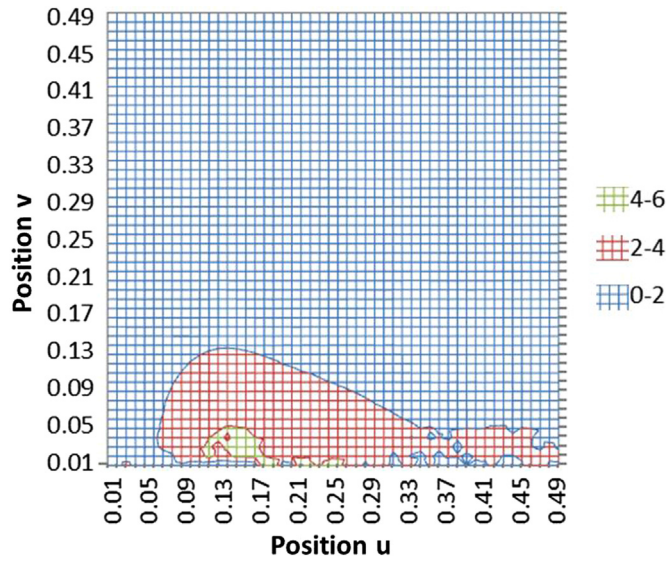
Fig. 3. Percentage error in position v for mass size equal to 0.25% of the mass plate.
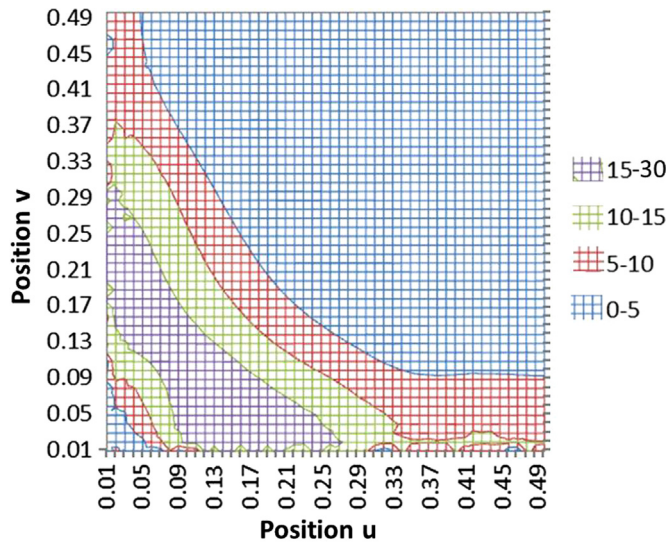
Fig. 4. Percentage error in mass identification for mass size equal to 0.50% of the mass plate.

$$\frac{C_{12}}{C_{11}} = 4\left(\cos^2 \frac{\pi y_0}{a} + \cos^2 \frac{\pi x_0}{a} \right),$$

(79)

$$\frac{C_{22}}{C_{11}} = 16 \ \cos^2 \frac{\pi y_0}{a} \ \cos^2 \frac{\pi x_0}{a}.$$

(80)

Let us define the position variables $Z = \cos^2 \frac{\pi x_0}{a}$, $W = \cos^2 \frac{\pi y_0}{a}$. Then, by (79) and (80), the variable Z solves the second-degree polynomial equation

$$X^2 - sX + p = 0, \quad s = \frac{C_{12}}{4C_{11}}, \quad p = \frac{C_{22}}{16C_{11}}.$$

(81)

By solving Eq. (81), we can find a closed form expression for the variable Z and, subsequently, for W. The solutions can be written as
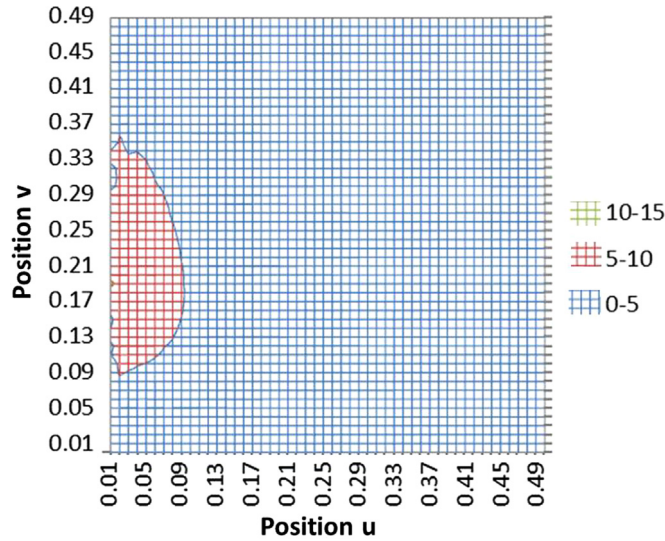
Fig. 5. Percentage error in position u for mass size equal to 0.50% of the mass plate.
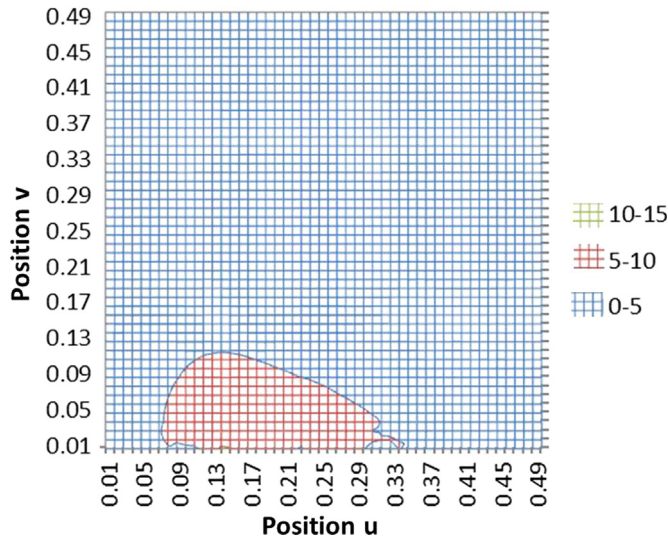
Fig. 6. Percentage error in position v for mass size equal to 0.50% of the mass plate.

$$\left\{ Z_1 = \frac{s - \sqrt{s^2 - 4p}}{2}, \quad W_1 = \frac{s + \sqrt{s^2 - 4p}}{2} \right\},$$

$$\left\{ Z_2 = \frac{s + \sqrt{s^2 - 4p}}{2}, \quad W_2 = \frac{s - \sqrt{s^2 - 4p}}{2} \right\},$$

(82)

Let us consider the solution $\{Z_1, W_1\}$ and let us denote by x_0^-, x_0^+ the x-coordinate values corresponding to Z_1 (i.e., $\cos^2(\pi x_0^\pm / a) = Z_1$), with $x_0^- < x_0^+$, and x_0^-, x_0^+ symmetric points with respect to $x = \frac{a}{2}$. Let us also denote by y_0^-, y_0^+ the two y-coordinate values corresponding to W_1 (i.e., $\cos^2(\pi y_0^\pm / b) = W_1$), with $y_0^- < y_0^+$ and y_0^-, y_0^+ symmetric points with respect to $y = \frac{a}{2}$. Therefore, the set of all the possible positions of the point mass associated to $\{Z_1, W_1\}$ is $\mathcal{P}_1 = \{(x_0^-, y_0^-), (x_0^+, y_0^-), (x_0^-, y_0^+), (x_0^+, y_0^+)\}$, which is a set of points symmetric with respect to the two axes $x = \frac{a}{2}$ and $y = \frac{a}{2}$. Let us consider the second solution $\{Z_2, W_2\}$. In this case, a direct inspection of the expressions of Z_2 and W_2 clearly shows that the role of the cartesian coordinates x and y is exchanged with respect to the previous solution $\{Z_1, W_1\}$. Then, the set of all the possible positions of the point mass associated to $\{Z_2, W_2\}$ is $\mathcal{P}_2 = \{(y_0^-, x_0^-), (y_0^+, x_0^-), (y_0^-, x_0^+), (y_0^+, x_0^+)\}$, which corresponds to positions of the point mass that are symmetrical of those belonging to the set $\mathcal{P}_1$ with respect to the diagonals of the square $(0, a) \times (0, a)$.
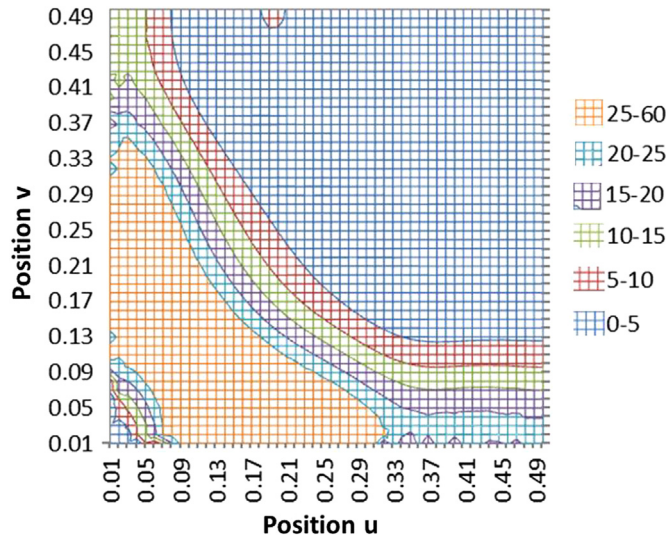
Fig. 7. Percentage error in mass identification for mass size equal to 1% of the mass plate.
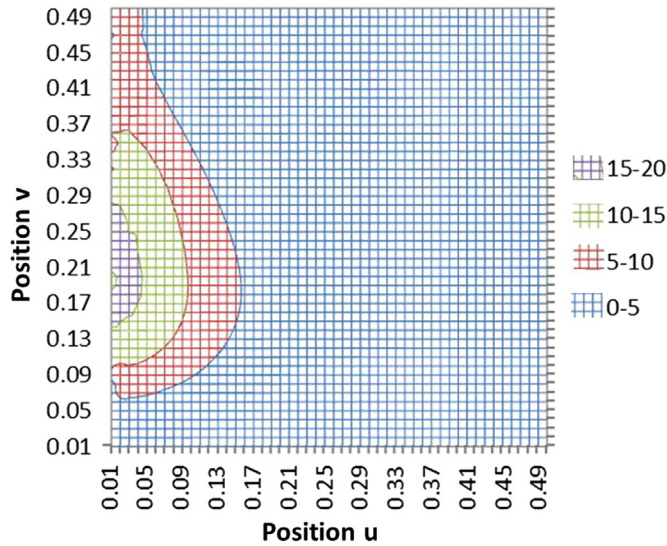
Fig. 8. Percentage error in position *u* for mass size equal to 1% of the mass plate.

Therefore, the additional symmetry of the square plate with respect to the diagonals makes the ill-posedness of the inverse problem more severe than the case of a proper rectangular plate. In fact, in order to recover uniquely the position of the point mass by three natural frequency values, here we need to operate on a $\frac{\pi}{4}$-angular sector of the square plate.

In conclusion, we notice that the application of the proposed identification technique to general domains is, in principle, possible. In fact, the analysis developed in Section 2 for the determination of the first order sensitivity of the eigenpairs holds for rather general domains, that is Ω can be a regular bounded domain in the plane. However, the extension of the identification method proposed in Sections 3 and 4 to a non-rectangular geometry faces with two additional difficulties. A first hindrance is connected with the absence of a closed-form expressions of the eigenfunctions of the unperturbed plate (even in the case of homogeneous isotropic linearly elastic material). A second – more important – difficulty is due to the fact that the first fundamental vibration mode may change sign and vanish somewhere inside Ω. It is possible to show that this occurs in a rectangular plate clamped at the boundary, see [11], and that there are similar examples for non-convex plane domains under simply supported boundary. This means that, in our notation, the quantity C_{11} may vanish in an internal point of the plate, and the identification procedure must be revised.
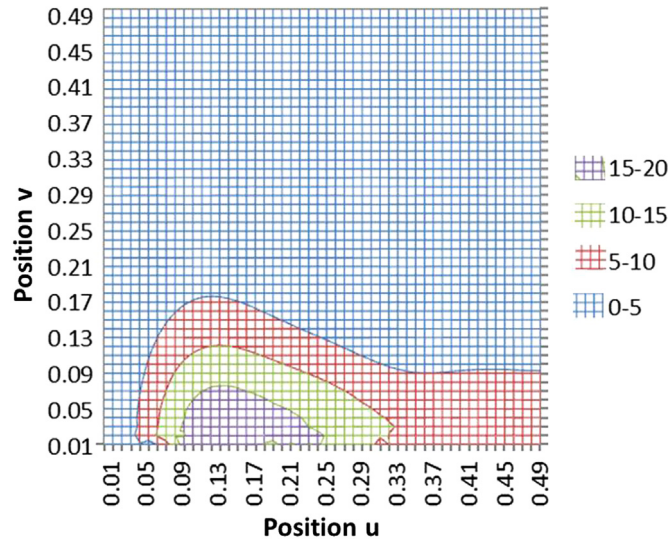
Fig. 9. Percentage error in position v for mass size equal to 1% of the mass plate.

Table 1

Simulations with errors on the frequency data: mass size $100 \times \frac{m}{\rho ab}$ and normalized positions $u = \frac{x_0}{a}$ and $v = \frac{y_0}{b}$ of the point mass; differences $d_{nm} = (\tilde{f}_{nm} - f_{nm})$ expressed in Hz.

Case	$100 \times \frac{m}{\rho ab}$	u	v	d_{11}	d_{12}	d_{21}
1a	0.25	0.176	0.153	−0.009	−0.084	−0.059
2a	0.25	0.354	0.196	−0.042	−0.319	−0.073
3a	0.25	0.110	0.384	−0.016	−0.023	−0.122
4a	0.25	0.261	0.375	−0.072	−0.117	−0.290
5a	0.25	0.422	0.334	−0.111	−0.311	−0.057
6a	0.25	0.412	0.431	−0.139	−0.072	−0.090
1b	0.50	0.176	0.153	−0.019	−0.169	−0.119
2b	0.50	0.354	0.196	−0.085	−0.636	−0.147
3b	0.50	0.110	0.384	−0.032	−0.046	−0.245
4b	0.50	0.261	0.375	−0.144	−0.231	−0.578
5b	0.50	0.422	0.334	−0.222	−0.318	−0.115
6b	0.50	0.412	0.431	−0.276	−0.144	−0.178
1c	1.00	0.176	0.153	−0.037	−0.344	−0.242
2c	1.00	0.354	0.196	−0.170	−1.267	−0.301
3c	1.00	0.110	0.384	−0.064	−0.092	−0.493
4c	1.00	0.261	0.375	−0.288	−0.448	−1.148
5c	1.00	0.422	0.334	− 0.441	−1.218	−0.233
6c	1.00	0.412	0.431	−0.547	−0.283	−0.352

5. Numerical examples and results

5.1. The specimen

This section is devoted to the presentation of a series of numerical simulations of the proposed identification technique. One goal of the analysis is the estimate of the limit of validity of the perturbation approach. A second objective concerns with the robustness of the method to errors on the input data.

Results of numerical simulations are presented for the simply supported steel plate considered in [3], with $a=0.8$ m, $b=1.0$ m, $h=0.005$ m, $E=210$ GPa, $\nu = 0.3$, volume mass density $\gamma = 7830$ kg m^{-3} ($\rho = \gamma h$). The first three natural frequencies $f_{nm} = \frac{\omega_{nm}}{2\pi}$ of the unperturbed plate are $f_{11} = 31.54$ Hz, $f_{12} = 68.47$ Hz, $f_{21} = 89.24$ Hz. By symmetry reasons, the point mass m is assumed to be placed in a quarter of the plate, precisely inside $Q = \{(x, y) \mid 0 < x < \frac{a}{2}, \; 0 < y < \frac{b}{2}\}$, and increasing mass sizes are considered.

Theoretical values of the first three natural frequencies of the plate with a point mass are obtained as zeros of the

Table 2
Simulations with errors on the frequency data: percentage errors $e_m = 100 \times (\bar{m}_{est} - m)/m$, $e_u = 100 \times (\bar{u}_{est} - u)/u$, $e_v = 100 \times (\bar{v}_{est} - v)/v$, where $\bar{m}_{est}$, $\bar{u}_{est}$, $\bar{v}_{est}$ are the average of m_{est}, u_{est}, v_{est}, respectively, and N is the total number of samples. Distribution 1.

Case	e_u	e_v	e_m	N
1a	80.80	105.62	44.00	29,542
2a	2.01	19.03	116.00	16,076
3a	149.36	−5.89	12.00	32,343
4a	−1.61	−0.65	192.00	11,532
5a	−2.27	−1.35	4.00	11,991
6a	−0.36	−1.72	0.00	12,813
1b	62.16	80.46	86.00	20,319
2b	0.65	2.60	108.00	11,944
3b	97.73	−1.77	134.00	25119
4b	−1.49	0.48	8.00	10,027
5b	−0.02	−0.09	0.00	10,254
6b	0.15	0.23	−2.00	10,295
1c	35.23	45.69	443.00	17,666
2c	−1.07	−1.43	160.00	10,170
3c	56.27	1.72	105.00	18,932
4c	0.50	1.09	−2.00	10,000
5c	−0.17	0.42	−2.00	10,000
6c	−0.02	0.19	−3.00	10,000

Table 3
Simulations with errors on the frequency data: percentage errors $e_m = 100 \times (\bar{m}_{est} - m)/m$, $e_u = 100 \times (\bar{u}_{est} - u)/u$, $e_v = 100 \times (\bar{v}_{est} - v)/v$, where $\bar{m}_{est}$, $\bar{u}_{est}$, $\bar{v}_{est}$ are the average of m_{est}, u_{est}, v_{est}, respectively, and N is the total number of samples. Distribution 2.

Case	e_u	e_v	e_m	N
1a	88.24	115.29	110.00	45,618
2a	0.08	40.56	100.00	22,607
3a	181.09	−8.44	56.00	43,748
4a	6.67	−2.96	132.00	16,460
5a	−7.39	−2.10	40.00	15,364
6a	−4.47	−6.66	16.00	18,494
1b	78.86	103.20	20.00	28,370
2b	1.44	17.14	120.00	15,486
3b	143.55	−5.73	28.00	30,937
4b	−2.18	−0.03	140.00	11,314
5b	−1.90	−0.87	4.00	11,668
6b	−0.15	−1.28	0.00	12,508
1c	60.17	76.41	98.00	20,154
2c	0.20	2.24	94.00	11,580
3c	92.64	−1.15	80.00	24,069
4c	−0.69	1.09	4.00	10,016
5c	−0.21	0.18	−2.00	10,182
6c	−0.17	0.28	−2.00	10,271

frequency equation

$$\frac{1}{4\lambda} = \xi \sum_{k,j=1}^{\infty} \frac{A_{kj}}{\lambda_{kj} - \lambda},$$

(83)

where $\xi = \frac{m}{\rho ab}$, λ_{kj} are the eigenvalues of the unperturbed plate and $A_{kj} = \sin^2(\frac{k\pi x_0}{a}) \sin^2(\frac{j\pi y_0}{b})$, see [12]. In order to solve (83), and after a careful comparison with the results obtained by taking an increasing number of terms on the right hand side, a truncated series for $k=6$ and $j=5$ was considered, the same truncation values that have been used in [3]. In addition, recalling (6), Eq. (83) was solved by means of a standard iteration algorithm with initial point taken coincident with the unperturbed value of every eigenvalue.

5.2. Results for error-free frequency data

We first present the results for frequency data free of error. Numerical simulations have been carried out by dividing both sides of the plate into 50 equally sized intervals, for a total of 2500 nodes, and the mass m was located at all nodes of the mesh. For each mass position, the normalized spatial variables $u = \frac{x_0}{a}$, $v = \frac{y_0}{b}$ and the mass size m were evaluated by Eqs. (73)–(75) (note that the first eight eigenvalues of the plate are simple in the present case). The percentage errors between estimated and actual values of the identification parameters are summarized in the three groups of Figs. 1–3, 4–6 and 7–9 for $\frac{m}{\rho ab} = \frac{0.25}{100}$, $\frac{m}{\rho ab} = \frac{0.50}{100}$ and $\frac{m}{\rho ab} = \frac{1}{100}$, respectively. For a better comprehension of the identification results, error contour curves are shown in these figures. In general terms, the estimation of the position variables u and v is more accurate than the estimate of the mass size m. The maximum percentage error for m is equal to 14, 26 and 56 percent for $\frac{m}{\rho ab} = \frac{0.25}{100}, \frac{0.50}{100}, \frac{1}{100}$, respectively, whereas the maximum discrepancy for u, v was respectively equal to 6, 11, 19 percent. Maximum errors on the position variables are attained near the edges of the plate, that is near $x = 0$ for v and near $y = 0$ for u, and the errors typically decrease quickly by approaching the interior points of the plate. Maximum errors on m were found for mass positions u, v approximately belonging to the region $u + v \leq 0.5$.

5.3. Results for noisy frequency data

In a second stage of the analysis, measurement errors are assumed to be present in frequency data. In particular, randomly generated errors are added to exact natural frequency values f_{nm} according to the equation

$$f_{nm}^{pert} = f_{nm} + \tau, \tag{84}$$

where τ is a real random Gaussian variable with zero mean. Two normal distributions with standard deviations $\sigma_1 = \frac{0.04}{3}$ Hz (Distribution 1) and $\sigma_1 = \frac{0.075}{3}$ Hz (Distribution 2) have been considered. Therefore, the maximum error magnitude is equal to 3σ, corresponding to ± 0.04 Hz and ± 0.075 Hz, respectively. These values are close to average errors found on frequency measurements in real experiments. Six different positions (x_0, y_0) of the point mass within the rectangular domain Q are considered, and the previous levels of mass size m, $\frac{m}{\rho ab} = \frac{0.25}{100}, \frac{0.50}{100}, \frac{1}{100}$ (cases a, b, c, respectively), are included in calculations. In Table 1, the coordinates $u = \frac{x_0}{a}$, $v = \frac{y_0}{b}$ of the selected positions and mass size m are displayed, together with the frequency changes induced by the point mass. For each combination of position and mass intensity, a Monte Carlo simulation on a population of 10,000 valid samples has been carried out. An identification sample is considered valid when the closed-form expressions (73)–(75) give admissible values of the identified parameters, namely, m positive and both u and v belonging to $(0, \frac{1}{2})$. Tables 2 and 3 show the errors in the estimations of the mass intensity and the positions u, v. The errors have been calculated with respect to the mean value of the position and mass size corresponding to the 10,000 valid samples. The tables also collect the number of samples N needed to reach 10,000 valid samples. It can be observed that the addition of random errors in the frequency data do not change the conclusions of the inverse problem solution in the absence of measurement errors, as the best results are obtained at positions far from the supported edges of the plate (see cases 4–6, for any mass intensity). On the other hand, larger values of N were typically necessary for masses located near the support edges of the plate. The comparison between Tables 2 and 3 shows as well that the accuracy of the identification gets better as the errors in the measurements are smaller. This behavior is in agreement with the findings of most of the identification methods based on natural frequency measurements, in which noisy errors on the data may be amplified strongly when their magnitude is comparable to the eigenfrequency shifts induced by the perturbation.

6. Conclusions

A perturbation approach has been applied to the determination of the location and the magnitude of a concentrated mass on a simply supported rectangular plate from natural frequency measurements. The analysis focussed on formulating and solving the inverse problem in terms of a minimal set of frequency data.

The method is based on the derivation of an explicit expression of the frequency sensitivity to a point mass and allows us to include the case of multiple eigenvalues. In particular, closed-form expressions for the mass size and the two position variables in terms of the first three natural frequencies are provided. Numerical results are in agreement with the theory when free-of-error data are employed in identification. In these cases, the estimate of the mass size is more sensitive to errors than the two position variables, and deviations are typically larger when the point mass approaches the boundary of the plate. A series of simulations performed on noisy data confirmed that, in the inverse problem solution, the errors on natural frequencies are usually amplified strongly when the point in close to the supported edges of the plate.

The present work is part of a more general long-term research project on detection of defects, such as holes, cracks and delamination, in plates by vibrational methods. In connection with this goal, further work is required, both from the theoretical and experimental/numerical point of view. The extension of the method to composite plates is another challenging issue that could be investigated. In this regard, it should be mentioned the recent contribution by Rajendran and Srinivasan [13] on the identification of an added mass in a glass fibre reinforced polymer composite plate by using a combination of

rotational mode shape information with wavelet transform analysis.

Acknowledgments

References

[1] A. Aydogdu, S. Filiz, Vibration analysis of symmetric laminated composite plates with attached mass, Mech. Adv. Mater. Struct. 23 (2) (2016) 136–145.
[2] A.J. McMillan, A.J. Keane, Shifting resonances from a frequency band by applying concentrated masses to a thin rectangular plate, J. Sound Vib. 192 (2) (1996) 549–562.
[3] W. Ostachowicz, M. Krawzuk, M. Cartmell, The location of a concentrated mass on rectangular plates from measurements of natural vibrations, Comput. Struct. 80 (2002) 1419–1428.
[4] A. Morassi, Identification of a crack in a rod based on changes in a pair of natural frequencies, J. Sound Vib. 242 (4) (2001) 577–596.
[5] R. Courant, D. Hilbert, Methods of Mathematical Physics, vol. I, First English Edition, Interscience Publishers, Inc., New York, 1966.
[6] T. Kato, Perturbation Theory for Linear Operators, Springer, Berlin, Germany, 1995.
[7] M. Amabili, M. Pellegrini, F. Righi, F. Vinci, Effect of concentrated masses with rotary inertia on vibrations of rectangular plates, J. Sound Vib. 295 (2006) 1–12.
[8] S. Jimbo, A. Morassi, G. Nakamura, K. Shirota, A non-destructive method for damage detection in steel-concrete structures based on finite eigendata, Inverse Probl. Sci. Eng. 20 (2) (2012) 233–270.
[9] A. Morassi, M. Dilena, On point mass identification in rods and beams from minimal frequency measurements, Inverse Probl. Sci. Eng. 10 (3) (2002) 183–201.
[10] A.M. Akhtyamov, A.R. Ayupova, Point mass identification in rods, Russ. J. Nondestr. Test. 49 (10) (2013) 572–578.
[11] V.A. Kozlov, V.A. Kondrat'ev, V.G. Maz'ya, On sign variability and the absence of 'strong' zeros of solutions of elliptic equations. Izv. Ross. Akad. Nauk. Seriya Mat. 53 (1989) 328–344 (in Russian); Translation in Mathematics of the USSR-Izvestiya 34 (1990).
[12] C.L. Amba-Rao, On the vibration of a rectangular plate carrying a concentrated mass, J. Appl. Mech. 31 (1964) 550–551.
[13] P. Rajendran, S.M. Srinivasan, Identification of added mass in the composite plate structure based on wavelet packet transform, Strain—An International Journal for Experimental Mechanics 52 (1) (2016) 14–25.